

# Status of Mechanistic Fission Gas Model in High-Burnup Fuel



Oliver Baldwin  
W. Cade Brinkley  
Charles Lieou  
Brian D. Wirth  
Nathan Capps

**September 2023**

## DOCUMENT AVAILABILITY

Reports produced after January 1, 1996, are generally available free via OSTI.GOV.

**Website** [www.osti.gov](http://www.osti.gov)

Reports produced before January 1, 1996, may be purchased by members of the public from the following source:

National Technical Information Service  
5285 Port Royal Road  
Springfield, VA 22161  
**Telephone** 703-605-6000 (1-800-553-6847)  
**TDD** 703-487-4639  
**Fax** 703-605-6900  
**E-mail** [info@ntis.gov](mailto:info@ntis.gov)  
**Website** <http://classic.ntis.gov/>

Reports are available to US Department of Energy (DOE) employees, DOE contractors, Energy Technology Data Exchange representatives, and International Nuclear Information System representatives from the following source:

Office of Scientific and Technical Information  
PO Box 62  
Oak Ridge, TN 37831  
**Telephone** 865-576-8401  
**Fax** 865-576-5728  
**E-mail** [reports@osti.gov](mailto:reports@osti.gov)  
**Website** <https://www.osti.gov/>

This report was prepared as an account of work sponsored by an agency of the United States Government. Neither the United States Government nor any agency thereof, nor any of their employees, makes any warranty, express or implied, or assumes any legal liability or responsibility for the accuracy, completeness, or usefulness of any information, apparatus, product, or process disclosed, or represents that its use would not infringe privately owned rights. Reference herein to any specific commercial product, process, or service by trade name, trademark, manufacturer, or otherwise, does not necessarily constitute or imply its endorsement, recommendation, or favoring by the United States Government or any agency thereof. The views and opinions of authors expressed herein do not necessarily state or reflect those of the United States Government or any agency thereof.

# **STATUS OF MECHANISTIC FISSION GAS MODEL IN HIGH-BURNUP FUEL**

Oliver Baldwin, University of Tennessee  
W. Cade Brinkley, University of Tennessee  
Charles Lieou, University of Tennessee  
Brian D. Wirth, University of Tennessee and Oak Ridge National Laboratory  
Nathan Capps, Oak Ridge National Laboratory

September 2023

Prepared by  
OAK RIDGE NATIONAL LABORATORY  
Oak Ridge, TN 37831  
managed by  
UT-BATTELLE LLC  
for the  
US DEPARTMENT OF ENERGY  
under contract DE-AC05-00OR22725



## CONTENTS

|  |     |
|--|-----|
| LIST OF FIGURES .....  | iii |
| LIST OF TABLES.....  | iii |
| ABBREVIATIONS .....  | iii |
| ABSTRACT.....  | 1   |
| 1. INTRODUCTION AND MOTIVATION .....   | 1   |
| 2. IMPROVED EXPERIMENTAL CHARACTERIZATION OF FISSION GAS BUBBLES IN<br>UO <sub>2</sub> LWR FUEL..... | 4   |
| 3. INITIAL TFGR MODEL .....  | 6   |
| 4. FRAMEWORK FOR MECHANISTIC TFGR AND MICROSTRUCTURAL EVOLUTION<br>MODELS .....                      | 8   |
| 4.1 MECHANISTIC TFGR MODELING FRAMEWORK.....   | 8   |
| 4.2 MECHANISTIC MICROSTRUCTURAL EVOLUTION MODELING FRAMEWORK.....                                    | 9   |
| 5. DISCUSSION OF DATA NEEDS AND RECOMMENDATIONS TO IMPROVE MODELS.....                               | 13  |
| 6. SUMMARY AND FUTURE WORK .....   | 14  |
| 7. REFERENCES .....  | 16  |

## LIST OF FIGURES

|  |    |
|--|----|
| Figure 1. Roadmap of ongoing and planned experimental and computational research activities toward developing a mechanistic fission gas model for high-burnup fuel. ....   | 3  |
| Figure 2. Optical microscopy examinations of the fuel cross-section of (a) North Anna 1 as-irradiated, (b) North Anna 1 post-LOCA, (c) North Anna 2 as-irradiated, and (d) North Anna 2 post-LOCA. ....  | 5  |
| Figure 3. Comparison of North Anna 1 as-irradiated (top panel) and post-LOCA (bottom panel) fuel samples at similar radial locations. ....   | 6  |
| Figure 4. Energy dispersive x-ray spectroscopy map of a sharp lenticular crack (pore) in North Anna 1 post-LOCA at $0.51 r/r_0$ , which shows the Xe and contributors to five-metal precipitates. ....   | 6  |
| Figure 5. Verification of implementing the empirical model into BISON for the conditions of the single-pellet transient test data in which the black solid line is the analytic fit of the empirical model and the blue circles are the BISON output at the temperatures denoted by the red circles for four burnup conditions. .... | 7  |
| Figure 6. BISON prediction of FGR compared with a high-burnup experiment performed in Noirot et al. (2014) during thermal anneal. ....   | 8  |
| Figure 7. Radially resolved grain diameter data obtained from detailed experimental characterization performed at Oak Ridge National Laboratory. ....  | 9  |
| Figure 8. Burnup and temperature profiles used for fitting. ....   | 10 |
| Figure 9. Grain diameter data plotted against local temperature and burnup fitted to sigmoidal forms. ....   | 11 |
| Figure 10. Fractional high-burnup structure predictions for each microstructural data type resolved by whether it was predicted by temperature or burnup. ....   | 12 |
| Figure 11. Averaged fractional high-burnup structure predictions. ....   | 12 |

## LIST OF TABLES

|   |    |
|---|----|
| Table 1. Available parameters for the North Anna and Limerick fuel pellet data on high-burnup structure formation. .... | 9  |
| Table 2. Microstructural values corresponding to 0% and 100% restructured fuel fraction. ....                           | 11 |

## ABBREVIATIONS

|       |   |
|-------|---|
| BWR   | boiling water reactor                         |
| DNB   | departure from nuclear boiling                |
| EDS   | energy-dispersive x-ray spectroscopy          |
| FFRD  | fuel fragmentation, relocation, and dispersal |
| FG    | fission gas                                   |
| FGR   | fission gas release                           |
| FIB   | focused ion beam                              |
| FMPs  | five-metal precipitates                       |
| HAADF | high-angle annular dark-field                 |
| HBR   | H.B. Robinson pressurized water reactor       |
| HS    | high-burnup structure                         |
| HBU   | high burnup                                   |
| LOCA  | loss-of-coolant accident                      |
| LWR   | light water reactor                           |
| NA1   | North Anna Unit 1                             |
| NA2   | North Anna Unit 2                             |
| NA3   | North Anna Unit 3                             |
| NRC   | Nuclear Regulatory Commission                 |
| ORNL  | Oak Ridge National Laboratory                 |
| RIL   | research information letter                   |
| S/TEM | scanning/transmission electron microscopy     |
| SATS  | Severe Accident Test Station                  |
| tFGR  | transient fission gas release                 |
| TKD   | transmission Kikuchi diffraction              |

## ABSTRACT

A desire to increase fuel burnup to decrease the cost of nuclear power plants has led to significant interest within the nuclear industry to develop improved understanding of high-burnup nuclear fuel microstructure and the potential for fuel fragmentation, relocation, and dispersal that contribute to burnup and safe operating limits. This milestone report describes joint research activities and program planning to develop mechanistic models for high-burnup  $\text{UO}_2$  microstructure, including both intra- and intergranular gas bubble populations and fission gas release, specifically associated with transient release. This model development is being extensively leveraged against a rapidly growing experimental database of high-fidelity electron microscopy characterization of commercial, light water reactor fuel in the as-irradiated condition as well as that following simulated loss-of-coolant test conditions. This report describes the status of model development, highlights recent microstructural data, and summarizes the data needs to complete initial development and experimental validation of mechanistic models of fission gas and microstructural evolution at high burnup, as well as transient fission gas release.

## 1. INTRODUCTION AND MOTIVATION

The US nuclear energy industry is seeking strategies to further reduce energy production costs for the existing fleet of nuclear power-generating stations. Roughly 20% of nuclear power plant operating costs are associated with the cost of fuel (NEI 2019). Costs are governed by reactor core design, which dictates the number of fresh fuel assemblies and fuel utilization. The cost of each fuel assembly is ultimately beyond the utilities' control. However, optimizing the core design presents an opportunity for significant operational savings. Historically, core design optimization was limited by the technical specifications outlined by the light water reactor (LWR) final safety analysis report (NEI 2019, EPRI 2019).

Core designs are primarily limited by departure from nuclear boiling (DNB) failure criteria occurring during an anticipated operational occurrence or dry-out for boiling water reactors (BWRs; NEI 2019, EPRI 2019). US LWRs that are unaffected by DNB or dry-out-related limitations are often affected by crud-induced power shifts, which limit power peaking factors (NEI 2019, EPRI 2019). These core design constraints affect nearly all US operating nuclear power plants and their ability to operate in a competitive energy market. However, addressing these issues will not completely liberate the economic restrictions the nuclear industry faces. The industry is considering increasing fuel utilization by extending fuel cycle lengths from 18 to 24 months. Such a cycle length extension necessitates extending burnup beyond 62 GWd/tU rod average and requires increasing the  $^{235}\text{U}$  enrichment limit beyond 5 wt %. A combination of core design and fuel utilization modifications could save nuclear power plants a substantial amount of money per cycle. However, both current regulatory guidance and numerous technical challenges must be addressed before such economic benefits can be realized.

Regulatory guidance is nuanced, primarily revolving around increasing both enrichment above 5 wt %  $^{235}\text{U}$  and the rod average burnup of the peak rods beyond 62 GWd/tU. In the near term, the industry can avoid regulatory restrictions through an exemption request while regulatory changes are being addressed in parallel. The largest technical challenges associated with burnup extension involve ensuring fuel integrity to avoid fuel fragmentation, relocation, and dispersal (FFRD; NRC 2021). FFRD was first observed in integral loss-of-coolant accident (LOCA) testing performed at the Halden reactor (Wiesenack 2013, 2015), which revealed a significant deviation between low-burnup and high-burnup (HBU) fuel performance under LOCA conditions; FFRD was also observed in semi-integral tests at Studsvik (NRC 2011, CFR 1974). Low-burnup fuel (<60 GWd/tU) under LOCA conditions has been observed to fragment into large pieces relative to the size of the cladding rupture (~4 mm), and the amount of fuel relocation within the balloon region was modest. However, the Halden and Studsvik tests of HBU fuel (>67 GWd/tU) showed that fuel pellets could pulverize into a sand-like consistency (Wiesenack



2013, 2015). A fraction of these much smaller particle fragments could axially relocate within the balloon region and be susceptible to ejection through the cladding rupture opening and into the reactor primary vessel. This phenomenon has since been termed FFRD (Raynaud 2012); it could invalidate aspects of the historical assumptions made to resolve licensing concerns related to core coolability, as described in 10 CFR Part 50.46 (NRC 2017a), as well as assumptions related to source term (NRC 2017b).

The US Nuclear Regulatory Commission has published a research information letter (RIL; NRC 2021) on its interpretation of FFRD experimental data that highlights important elements for consideration in subsequent safety cases. The RIL highlights five factors that provide the technical basis for each element: (1) threshold for fine fragmentation, (2) cladding strain threshold for fuel relocation, (3) mass considered dispersible, (4) transient fission gas (FG) release (tFGR) and its effect on cladding balloon-burst behavior, and (5) packing fraction in the balloon region. Many of these factors have a well-established experimental database or test plans that can be used to further investigate the element in question. However, tFGR is a complex phenomenon that may have a wide-ranging effect on fuel performance and FFRD safety cases. Furthermore, integral tFGR data and consensus on the appropriate experimental approach and interpretation of the data are lacking.

The University of Tennessee and Oak Ridge National Laboratory (ORNL) hosted a 2-day US workshop in November 2022 to (1) evaluate the current experimental database and modeling capabilities for FG bubble formation and release in HBU nuclear fuel and (2) define a roadmap of activities. Subsequently, ORNL hosted a 2-day United States–France collaborative workshop on HBU fuel in June 2023. Those workshops have informed a roadmap of activities required to develop a mechanistic tFGR model, as shown in Figure 1 (Capps et al. 2023). Developing a mechanistic tFGR model requires knowledge of FG bubble distribution as a function of the fuel pellet radius resolved at the microstructure level and a coordinated research effort that involves computational modeling and experimental activities. The microstructure level resolution is needed because the distribution of gas bubbles within grains and on grain boundaries, combined with their gas content and volume, govern the propensity to induce fine fragmentation of the fuel pellet during transient events. The term *fine fragmentation* refers to fragments on the order of ~100–200 nm in diameter or smaller and distinguishes the phenomenon from the large fragmentations that occur for burnups <60 GWd/tU, which results in fragment sizes in the millimeter range. Fine fragmentation has been hypothesized to be responsible for tFGR.

In addition to tFGR linked to fragmentation and microcracking, FG may be released during steady state operation via diffusion to grain boundaries and interlinking of gas bubbles to form percolation networks, enabling the gas to reach triple junctions and free surfaces and then escape the pellet. This mechanism is the classical gas release mechanism predominant in UO<sub>2</sub> fuel at both steady state and temperature transient conditions where the fuel temperatures are sufficiently high (>~1,000°C). However, as the fuel reaches a sufficiently HBU (~40–50 GWd/tU), the lower temperature transient release mechanism described above can contribute to release during transient conditions. Further complicating understanding, the grain structure evolution is driven by burnup, irradiation, stress, and temperature effects. For example, the formation of small grains in UO<sub>2</sub> as a function of burnup may occur through the growth of dislocations into networks that form subgrain boundaries or enable recrystallization. The first phenomenon is due to irradiation-induced point defects agglomerating into large-scale defects, whereas the second is due to damage accumulation leading to a high driving force to remove defects by forming new grains and thus annihilate any lattice defects. Historical debate has occurred over which of these two mechanisms best describes the observed behavior of UO<sub>2</sub> exposed to HBU conditions. Recent evidence suggests that the more appropriate viewpoint may be to consider under what conditions one of these mechanisms dominates over the other and how they are connected (Rondinella and Wiss 2010). Small grains are believed to coincide with risk of fine fragmentation whether they occur in the HBU rim region or toward the pellet center (Seibert, Capps et al. 2022). Ultimately, we propose a hypothesis that the formation of inter- and intragranular FG bubbles in similar sizes and densities in different spatial regions

can result in subgrain formation and microstructure that is susceptible to fragmentation and tFGR. This behavior is theorized to persist until fuel temperatures are sufficiently high (closer to the fuel centerline) to promote  $\text{UO}_2$  bulk and grain deformation mechanisms (e.g., grain growth, creep, hot pressing, FGR) that effectively thermally anneal the irradiation effects and defected microstructures that are susceptible to fuel fragmentation and tFGR. For the appearance of small grains related to subgrain formation and the mechanism related to recrystallization, both mechanisms are driven by irradiation damage caused by point defects and their agglomeration into dislocations and voids or bubbles.

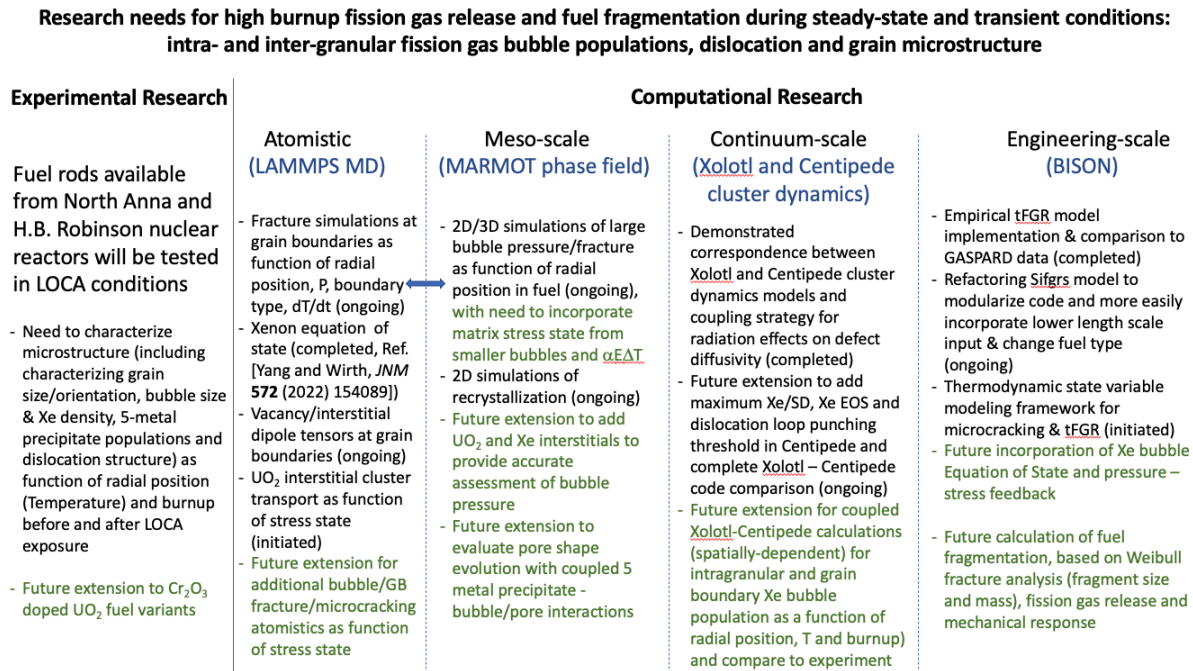


**Figure 1. Roadmap of ongoing and planned experimental and computational research activities toward developing a mechanistic fission gas model for high-burnup fuel.**

Reproduced from Capps et al. (2023).

There is an opportunity to expand existing cluster dynamics capabilities for  $\text{UO}_2$ , such as those embodied in the Centipede (Matthews et al. 2019) and Xolotl (Blondel et al. 2018) codes, to account for evolution of dislocations, dislocation networks, and eventually subgrain boundaries. These models must be parameterized by atomic-scale simulations. Independently, recrystallization models could be improved, particularly by adding more mechanistic descriptions of the lattice damage formation that drives recrystallization; this could be accomplished by phase field simulations (e.g., those enabled by the MARMOT code; Tonks et al. 2012) informed by atomic-scale parameters and possibly by other lower-length scale techniques. It is important to include vacancies, interstitials, and gas species in such phase field models.

After refining models to predict grain structure formation and evolution, the distribution of FG within grains, on dislocation networks, and on grain boundaries should be considered. This consideration should include separating bubbles into populations of different sizes, depending on microstructure location (intra- or intergranular bubbles or bubbles pinned at dislocations). The number density and pressure of each bubble population should be tracked to link them to fragmentation. Such an activity involves both mesoscale and engineering-scale model development, combined with extensive experimental characterization of the HBU fuel microstructure, including bubbles, second phase precipitates, dislocations, and the grain structure, along with efficient data analysis to enable cross-comparison and

validation of models. The bubble populations must eventually be tracked at the fuel performance level, but the simplifications necessary at the engineering scale should be verified by mesoscale simulations that use techniques such as spatially dependent cluster dynamics and phase field models. In particular, there is an opportunity for advanced cluster dynamics models of FG atom, gas bubble, and point defect phase space to perform simulations of bubble size distributions and pressures as a function of operating conditions and pellet radius; this can be experimentally validated against high fidelity transmission electron microscopy characterization of HBU commercial fuel as a function of position within the pellet and fuel rod.

The remainder of this milestone report discusses recent progress in developing advanced experimental data on FG bubble populations in HBU, commercial LWR fuel at ORNL, and the modeling framework envisioned to improve the fidelity of FG models. Subsequently we will discuss and prioritize numerous data needs and recommendations to improve the models.

## **2. IMPROVED EXPERIMENTAL CHARACTERIZATION OF FISSION GAS BUBBLES IN UO<sub>2</sub> LWR FUEL**

Under steady-state irradiation, UO<sub>2</sub> fuel undergoes intense microstructural changes, and with the prospective design of increasing fuel cycle lengths, analysis of fuel experiencing HBU conditions is required. Understanding the changes in HBU fuel from steady-state and transient conditions requires advanced microscopy techniques to examine grain structure, FG bubble nucleation, and behavior as a function of pellet radius. In the experimental observations, characterization is performed on three HBU commercial LWR UO<sub>2</sub> fuel rods. Multiple fuel samples were harvested from the North Anna Unit 1 (NA1), North Anna Unit 2 (NA2), and H. B. Robinson (HBR) pressurized water reactors, which reached an averaged rod burnup of 63, 68.5, and 66.5 GWd/tU, respectively. To simulate LOCA microstructural conditions, NA1 and NA2 fuel rod segments were subjected to LOCA testing in the Severe Accident Test Station (SATS) at ORNL. The SATS provides a unique capability of exposing irradiated fuels in extreme accident scenarios to further develop and analyze new fuel concepts.

Initial optical micrographs demonstrating the fuel cross-section microstructure of the as-irradiated and post-LOCA tested North Anna fuel samples are provided in Figure 2 (Seibert, McKinney et al. 2022). Previous observations identified five radial regions (high-burnup structure [HBS], HBS transition, mid-radial, central restructured, and central) with various microstructural behaviors across the fuel radius (Seibert, McKinney et al. 2022). Seibert, McKinney et al. (2022) previously reported that the porosity generally decreased with an increase in pore area from the fuel periphery to the center. However, there was a slight increase in porosity within the central restructured region, which corresponds to the dark ring viewed in Figure 2, then porosity dropped again closer to the pellet center. Between the as-irradiated and post-LOCA tested samples, there is a clear distinction observed due to the increase in pulverization and fragmentation near the pellet periphery and mid-radial region for the post-LOCA samples. For more advanced characterizations of these pores, the as-irradiated and post-LOCA tested fuel samples were prepared by a ThermoFisher Scios2 DualBeam focused ion beam (FIB) and then examined using the ORNL Talos F200X scanning/transmission electron microscopy (S/TEM) machine with energy-dispersive x-ray spectroscopy (EDS) methods to identify FG bubbles.

Results from the S/TEM and EDS characterization on the NA1 as-irradiated and post-LOCA fuel samples have been achieved and are presented in this work. NA2 as-irradiated examinations have been conducted, but the NA2 post-LOCA characterizations are currently ongoing. High-angle annular dark-field (HAADF) images were obtained for NA1 as-irradiated and post-LOCA at three similar radial locations in the fuel and are shown in Figure 3. In the top row of Figure 3, the NA1 as-irradiated HAADF images demonstrate visible grain structure and an increase in cavities as the location transitions closer to the center of the fuel. This cavity growth at  $0.57 r/r_0$ , where  $r$  is the radial location and  $r_0$  is the initial fuel

radius, and at  $0.53 r/r_0$  coincides with the initial observation of a porosity increase in the central restructured region. S/TEM analysis verified the presence of xenon bubbles in the as-irradiated sample inter- and intragranularly at various radial positions; these bubbles are commonly associated with a combination of five metals (Mo, Tc, Ru, Rh, and Pd), named five-metal precipitates (FMPs). The formation of FMPs does not negatively alter fuel performance properties. The xenon bubble distribution did not present an identifiable pattern and was located nonuniformly within the fuel.

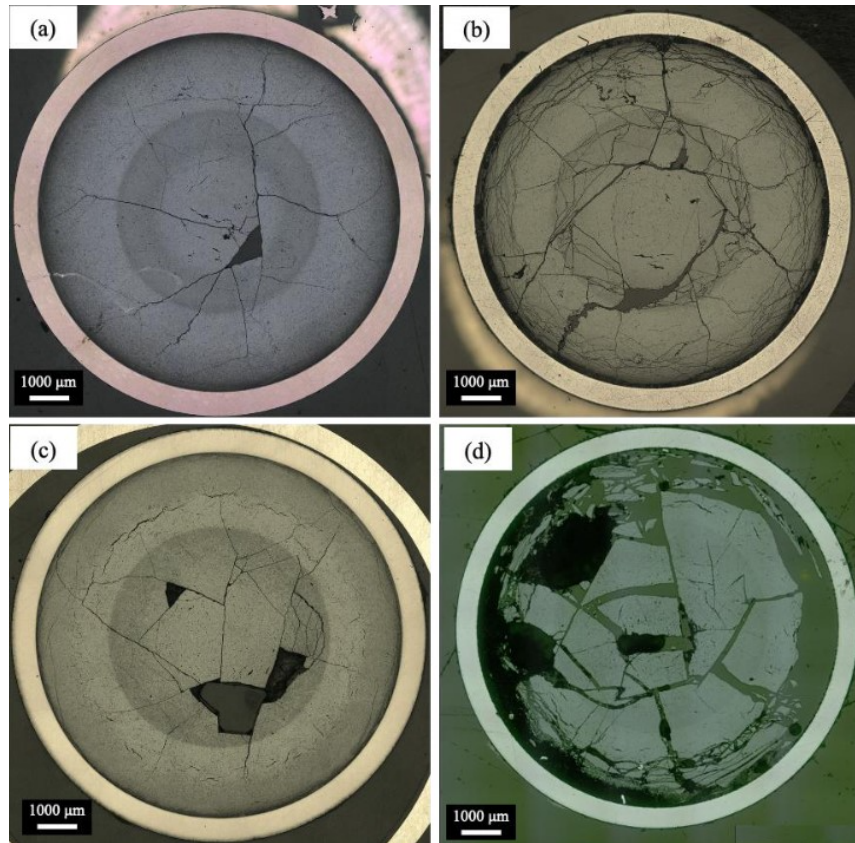


**Figure 2. Optical microscopy examinations of the fuel cross-section of (a) North Anna 1 as-irradiated, (b) North Anna 1 post-LOCA, (c) North Anna 2 as-irradiated, and (d) North Anna 2 post-LOCA. Reproduced from Seibert, McKinney et al. (2022).**

The bottom row of Figure 3 displays the NA2 post-LOCA HAADF images that follow the same trend as the as-irradiated fuel but contain a more significant growth in cavities as the fuel moves into the central restructured region. Another difference observed is that the grain structure is less apparent in all three images. However, this could be due to a larger sample thickness affecting the transparency in the S/TEM. At  $0.57$  and  $0.51 r/r_0$  of the post-LOCA data, there are noticeable differences in the cavities formed where the shape and size appear more lenticular and smaller compared with the appearance of the as-irradiated pores. These sharp lenticular bubbles are designated as tears and are highlighted by the red arrow in Figure 3. An EDS map of a singular tear in the NA1 post-LOCA fuel sample at  $0.51 r/r_0$  is presented in Figure 4. An interesting observation is the low xenon concentration surrounding the tear, which can be viewed as a denuded zone. FMPs are present mainly below the lenticular tear, but the distribution of FMPs in HBU fuel is still unknown.

Comparing the as-irradiated and post-LOCA data of NA1 demonstrates a need for more extensive microstructural characterizations to develop a deeper understanding of the distribution of FG bubbles and the presence of lenticular tears after LOCA testing. Additional S/TEM and EDS analysis is ongoing for the remaining North Anna samples, and transmission Kikuchi diffraction (TKD) is planned to analyze crystallographic features to better understand this behavior.



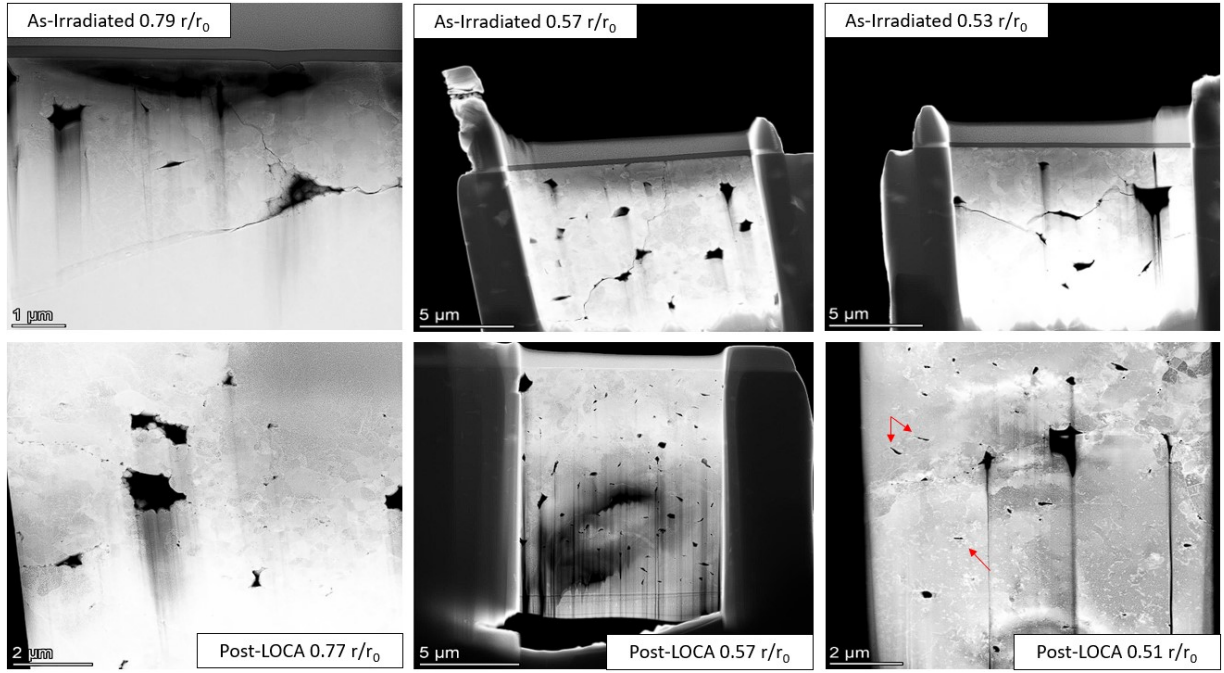


**Figure 3. Comparison of North Anna 1 as-irradiated (top panel) and post-LOCA (bottom panel) fuel samples at similar radial locations.**

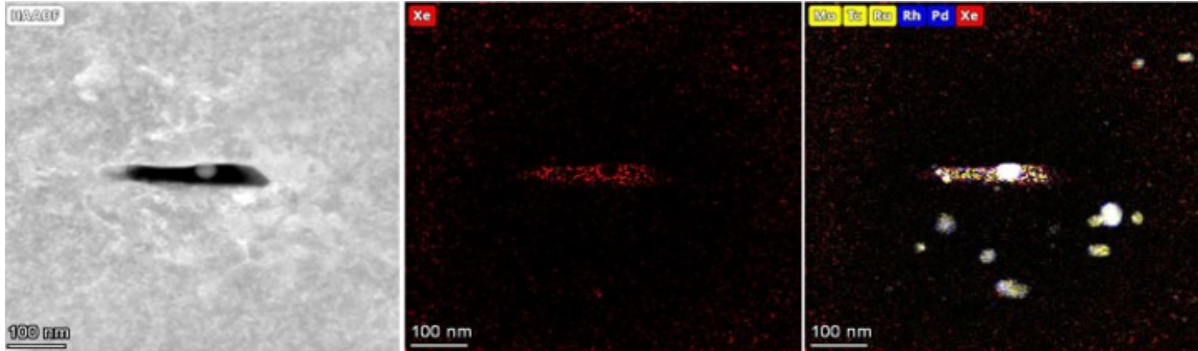


**Figure 4. Energy dispersive x-ray spectroscopy map of a sharp lenticular crack (pore) in North Anna 1 post-LOCA at 0.51  $r/r_0$ , which shows the Xe and contributors to five-metal precipitates.**

### 3. INITIAL TFGR MODEL

An initial empirical model for tFGR has been performed using a double sigmoidal function and fit to data identified from French datasets by Capps et al. (2023). This new empirical tFGR model has been included as an option in the SIFGRS module of BISON, although the details of the model are not presented here in the interest of brevity. Interested readers are referred to Capps et al. (2023). Three simulations were prepared to confirm that the model implemented in BISON was accurately calculating the FGR consistent with the empirical model. These simulations were for burnups identical to the single-pellet annealing data cases with representative base irradiation power profiles and subsequent accelerated heating rates corresponding to the experimental conditions. Figure 5 compares the analytic empirical model (black solid line) to the implemented version in BISON (blue circles) as a function of time, for which  $t = 0$  s denotes the start of the transient heating test. The red circles denote the temperature profile input to

BISON. The agreement between the analytic model (Figure 5) and the BISON output is excellent, indicating that the empirical model was implemented successfully into the SIFGRS module.

Subsequently, the BISON model and experimental data were directly compared. The base irradiation was simulated using a representative pressurized water reactor power history up to the burnup level of the standard single-pellet experiments, followed by a heating ramp. Overall, the new empirical model provides a reasonable agreement with the experimental results, although the model underpredicts the FG release for a burnup of 48.5 GWd/tU. Subsequently, additional data were identified to evaluate the model predictions at a burnup of 103.5 GWd/MtU (Noirot 2014) and, unlike the single-pellet data, were derived from a  $\text{UO}_2$  disk irradiated in the Halden BWR. The burnup and temperature profile in the sample are expected to be nearly uniform. The stresses on the fuel disk are expected to be near zero as well. A fuel pellet will have both a temperature and a burnup gradient across the pellet radius, resulting in high stress gradients and cracking. Other impacts such as fission rate and steady state FG release will affect the results, as well; however, a true physics-based model should be able to capture this behavior. Figure 6 compares the experimental data and BISON-calculated FGR using the newly fit empirical model. As indicated, the BISON prediction indicates higher initial FGR relative to the experimental data during the first 4,000 s of the test and predicts a plateau in the magnitude of the FGR that is lower than the experimental from Noirot et al. (2014). It will be important to further compare this new model to additional experimental data in the future; however, this comparison motivates the development of a mechanistic-based model to predict tFGR in addition to further experimental data and detailed microstructural characterization, as discussed in the following sections.

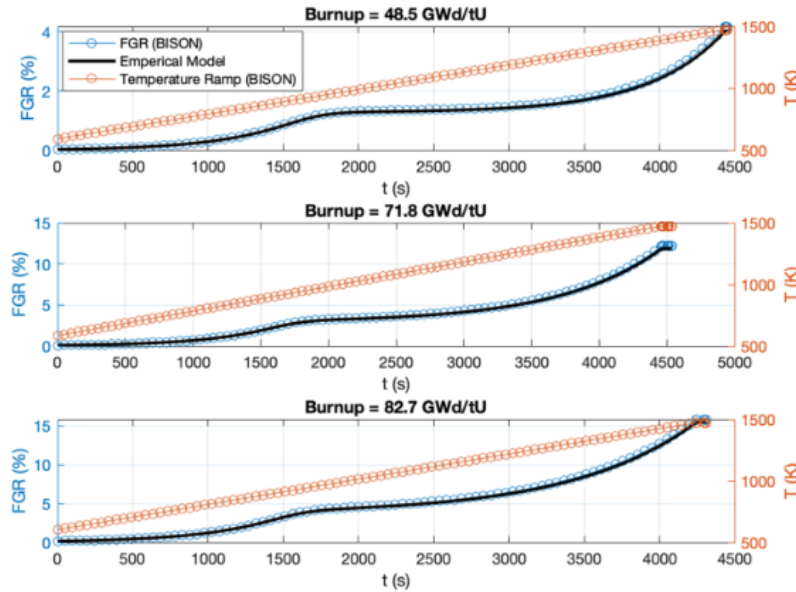


**Figure 5. Verification of implementing the empirical model into BISON for the conditions of the single-pellet transient test data in which the black solid line is the analytic fit of the empirical model and the blue circles are the BISON output at the temperatures denoted by the red circles for four burnup conditions.**

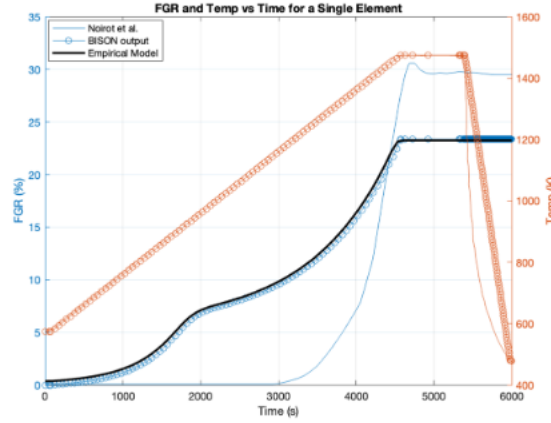


**Figure 6. BISON prediction of FGR compared with a high-burnup experiment performed in Noirot et al. (2014) during thermal anneal.** Blue circles represent the BISON output at the temperatures denoted by the red circles, blue solid lines represent the experimental fission gas release, and red solid lines represent the temperature data.

#### 4. FRAMEWORK FOR MECHANISTIC TFGR AND MICROSTRUCTURAL EVOLUTION MODELS

##### 4.1 MECHANISTIC TFGR MODELING FRAMEWORK

Here, we briefly describe a thermodynamic approach that represents the kinematics and dynamics of microcracking with internal state variables that are representative of the fuel microstructure in a statistically meaningful manner, and which we believe provides a framework for a mechanistic tFGR model. In our model, we expand on the traditional approach (Pastore 2013) to describe intragranular xenon bubble evolution and the transport of FG to grain boundaries where grain face bubbles can give rise to both coalescence and percolation driving steady-state FG release and a microcracking mechanism that can produce transient release.

Our proposed model focuses on the kinematics of grain-face microcracking and FG release and diverges from the traditional model described by Pastore et al. (2013). The basic idea within this modeling framework is that microcracking reduces the grain face gas storage capacity and provides a network through which FG stored in intergranular bubbles can be released. This framework involves a statistical thermodynamic description of defects and their development under mechanically nonequilibrium conditions, within the constraints of the second law of thermodynamics. The basic idea is that internal defects, including grain boundaries, microcracks, and grain face bubbles, can be described by well-defined internal state variables representing respective densities over a macroscopic length scale that is macroscopically small but much larger than the atomic size. The presence of these defects contributes both enthalpy and entropy, and the defect evolution can then be described by the principle of dynamical free energy minimization.

Again, in the interest of brevity, the system of equations describing this approach will not be presented here but will be the subject of a forthcoming manuscript that has been submitted to the *Journal of Nuclear Materials* (Lieou 2023). The data developed and analyzed within this project will contribute extensively to this modeling framework.

## 4.2 MECHANISTIC MICROSTRUCTURAL EVOLUTION MODELING FRAMEWORK

Macroscale behaviors such as FGR and FFRD depend on the fuel microstructure. This makes the development of an appropriate computational model for microstructure evolution (whether mechanistically or empirically based) an important step in cost-effectively predicting the behavior of fuel at HBU. Recent radially resolved characterization efforts of  $\text{UO}_2$  pellets from NA1, NA2, and NA3, as well as Limerick (Seibert, McKinney et al. 2022; McKinney et al. 2023) have provided a basis for developing a preliminary model for microstructure evolution that informs a prediction of a volumetric fraction of HBS at any radial position in a fuel pellet. Radially resolved microstructural data have been provided characterizing pore number density, pore area, grain diameter, and high-and low-angle grain boundary length per unit area. Figure 7 provides an example of the data (Seibert, McKinney et al. 2022; McKinney et al. 2023).

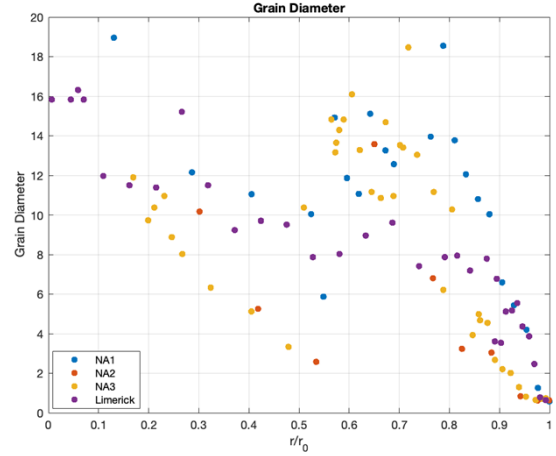


**Figure 7. Radially resolved grain diameter data obtained from detailed experimental characterization performed at Oak Ridge National Laboratory.** From Seibert, McKinney et al. 2022 and McKinney et al. 2023.

Microstructural data are fit against local burnup and temperature, with room for expansion to other relevant parameters as they become apparent. In the absence of precise power histories for each pellet, estimations of temperature and burnup histories must be developed. Available information about the power histories of the characterized pellets is shown in Table 1.

**Table 1. Available parameters for the North Anna and Limerick fuel pellet data on high-burnup structure formation**

| Sample            | Pellet average burnup (GWd/tU) | Last cycle power (kW/m) | Pellet radius (mm) |
|-------------------|--------------------------------|-------------------------|--------------------|
| North Anna unit 1 | 69                             | 19–23                   | 4.21               |
| North Anna unit 2 | 77                             | 19–23                   | 4.30               |
| North Anna unit 3 | 75                             | >15                     | 4.10               |
| Limerick          | 63.5                           | 16–17                   | 4.78               |

Sources: Seibert, McKinney et al. 2022; McKinney et al. 2023.

Constructing a temperature profile from the linear heat rate  $q_L$  is straightforward if the fuel surface temperature  $T_o$  and pellet radius  $r_o$  are known. In these cases, it was estimated to be 690 K. The profile is given by Equation (1) below.

$$T(r) = \frac{q_L}{4\pi k} \left( 1 - \frac{r^2}{r_o^2} \right) + T_o(1)$$



The approximate shape of the burnup profile  $f(r)$  for pellet fuel is known from Lassmann (1994). The pellet average burnup  $\beta_{avg}$  is known and can be used to scale the Lassmann equation using multiplier B as shown in Equations (2a) and (2b). The burnup and temperature profiles used are plotted in Figure 8.

$$f(r) = 1 + p_1 \exp(-p_2(r_0 - r)^{p_3}) \quad (2a)$$

$$\beta_{avg} = \frac{B}{\pi r_0^2} \int_0^{2\pi} \int_0^{r_0} f(r) r dr d\theta \quad (2b)$$

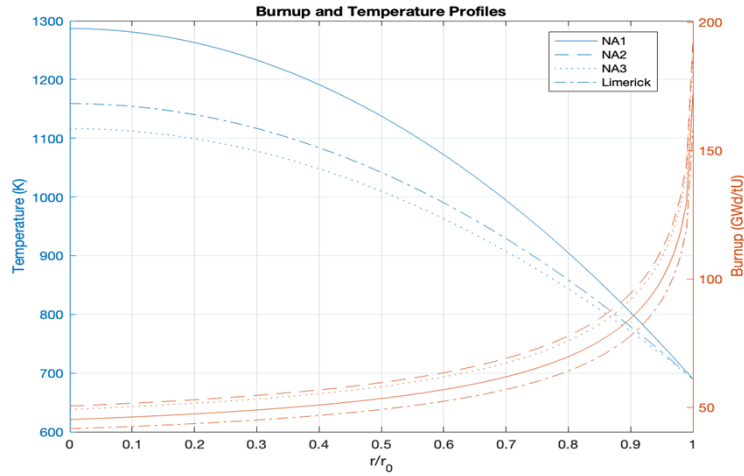


**Figure 8. Burnup and temperature profiles used for fitting.**

To develop correlations as functions of temperature and burnup, the raw microstructural data must be arranged such that each microstructural data point corresponds to a local temperature and burnup from the profiles described here. This is accomplished by using a MATLAB script that looks up a corresponding temperature and burnup history using the radial location, average burnup, and linear heat rate for each data point. Once the data are resolved against temperature and burnup, a fit is developed for each data type using least squares regression for a chosen form of equation. Figure 9 shows an example of the output of this process for grain diameter, which is shown fitted to a sigmoidal type equation. Fits for each data type will be refined as more sophisticated physically based forms are adopted.

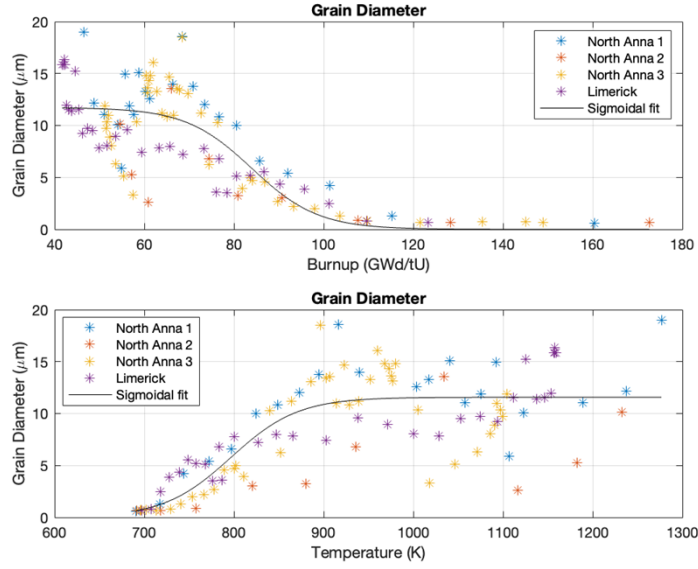


**Figure 9. Grain diameter data plotted against local temperature and burnup fitted to sigmoidal forms.**

Predicting a volumetric restructured fraction of the fuel pellet requires quantitatively defining how microstructure relates to HBS. A simple approach was adopted for preliminary calculations where, for each microstructural data type, values were defined to correspond to 0% and 100% restructuring. These defined values are reported in Table 2. The final restructured fraction for a radial position is calculated by averaging across all data types for both temperature and burnup.

**Table 2. Microstructural values corresponding to 0% and 100% restructured fuel fraction**

|                    | Number of pores | Grain diameter (μm) | LAGB length (μm) | HAGB length (μm) | Pore area (μm <sup>2</sup> ) |
|--------------------|-----------------|---------------------|------------------|------------------|------------------------------|
| 0% restructuring   | 0               | 12                  | 0.25             | 0                | 0                            |
| 100% restructuring | 800             | 0.1                 | 1.5              | 3                | 700                          |

LAGB = Low Angle Grain Boundary; HAGB = High Angle Grain Boundary

The raw microstructural data from McKinney et al. (2023) have been used to isolate the correlation between microstructure characteristics and HBS. The individual microstructural predictions are averaged for each radial position for temperature and burnup both individually and as a total mean prediction. If a microstructural characteristic predicts a restructured fraction outside of the 0%–100% window, it is kept in the average but is not shown in the plot, which is clipped to only physically valid regions. A manufactured representative power history was constructed to demonstrate the ability of the model to go from a power history to HBS fraction by utilizing microstructural predictions. The output from the equations fitted to microstructural data are fed into the microstructure-to-HBS correlation to produce the graphs in Figures 10 and 11.

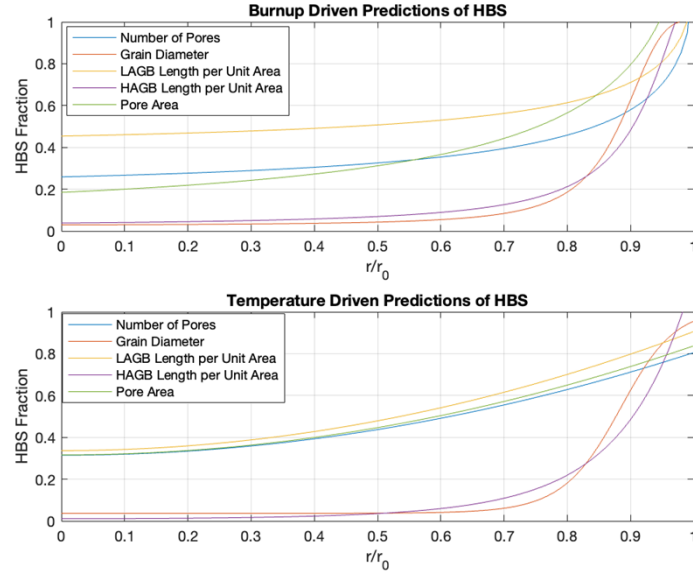


**Figure 10. Fractional high-burnup structure predictions for each microstructural data type resolved by whether it was predicted by temperature or burnup.**

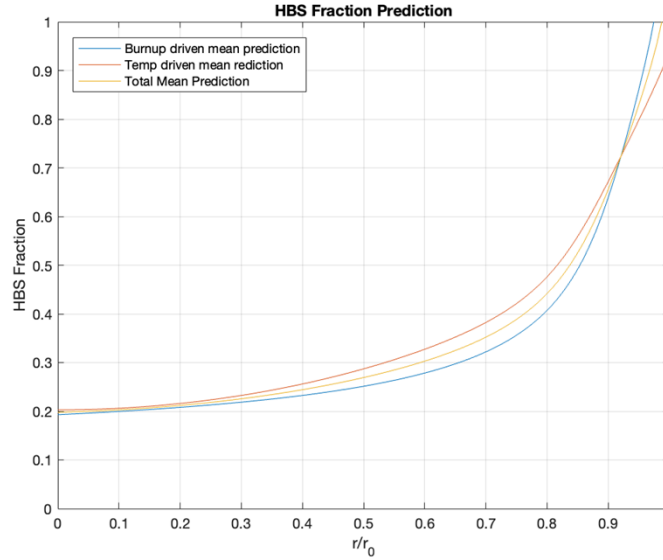


**Figure 11. Averaged fractional high-burnup structure predictions.**

The predictions in Figures 10 and 11 demonstrate an ability to predict HBS fraction from a power history, but the predictions are less consistent with experimental observations (McKinney et al. 2023) than with the predictions directly from microstructural data. Recent observations show a region of restructuring around 0.3–0.5  $r/r_0$  that has been dubbed the central restructured region. This comparison highlights that the key to predicting the central restructured region lies in the quality of the experimental data available to provide mechanistic models for the microstructural data, combined with detailed power histories.

The immediate focus of future work is the refinement of the fits of microstructure to power histories. These fits will be mechanistically informed, allowing for accurate prediction of a variety of physical

phenomena. Additionally, knowing exact power histories for the North Anna data would be ideal, but a satisfactory substitute would be the output from a representative BISON fuel performance simulation. The final improvement to this model would be reformulation as a differential equation, which would allow validity at any time step in a simulation.

## **5. DISCUSSION OF DATA NEEDS AND RECOMMENDATIONS TO IMPROVE MODELS**

As noted in the introduction and presented in Figure 1, both motivation and a significant opportunity exist to develop improved material models for  $\text{UO}_2$  fuel, in particular predictive models for radially resolved FGR calculations and HBS evolution. Pursuant to the development of these models, there are notable data needs for radially resolved microstructure data, such as resolved cavities within the fuel matrix and along grain boundaries; gas evolution including generation, nucleation, growth, re-resolution, and coalescence of bubbles; and FGR.

Characterization of fuel across the radius of the pellet will allow for improved understanding of the dependence of microstructural evolution and restructuring on the local burnup and temperature. The development of improved material models is further motivated by the opportunity for significantly improved and high-fidelity experimental data from SATS, which has integral LOCA testing capabilities for pre-irradiated fuel and is being used in the development of a growing experimental database.

With an increased ability to develop a correlation between local fuel conditions and microstructure comes the possibility of developing mechanistic and semi-empirical models for  $\text{UO}_2$  fuel FGR and HBS development. To describe the restructuring behavior, data needed include pore number density, pore area, grain size, high-angle grain boundary length and area, and low-angle grain boundary length and area. Changes in each of these parameters are known to be observed in the formation of HBS. As such, to describe the observed restructuring behavior, it is necessary to provide a model that describes not only the radial dependence of these parameters but also how the radial data change during reactor operation.

Improved material models are useful to predict macroscopic reactor behavior. Although radially resolved data exist for fuel pellets at the end of life, particularly at HBU (69 and 77 GWd/MtU for NA1 and NA2, respectively), similarly resolved data are not available for lower-burnup pellets or fresh fuel. There is motivation to fill a data gap associated with the microstructure of lower-burnup fuel and to perform characterization of fresh  $\text{UO}_2$  fuel. Material models, particularly mechanistic models, require an understanding of fuel initial characteristics to properly represent the change in the material properties and garner a more cohesive understanding of the restructuring behavior of the fuel. As such, the burnup dependence of the evolution of parameters of interest is based on assumptions made about the initial conditions of fuel microstructure. Performing characterization on fresh and lower-burnup fuel will reduce the assumptions required for model development and improve the fidelity of models.

Fresh fuel characterization will close the data gap associated with initial conditions of the fuel microstructure, whereas lower-burnup fuel characterizations will allow for an understanding of the form of burnup dependence for restructuring behavior. The restructuring behavior is observed and parameterized through pore number density, pore area, grain size, high-angle grain boundary length and area, and low-angle grain boundary length and area. Following characterization of the microstructure, these parameters can be used to conceptualize restructuring the fuel into HBS.

A preliminary model of grain diameter changes highlights deficiencies in the assumptions made in developing new material models. A radially resolved model for grain diameter evolution would likely contain grain growth at high temperatures and grain shrinkage at HBU. The available data allow for an excellent prediction of the radially resolved end-of-life grain diameter, but there are no data on the grain diameter during burnup or at the start of pellet life. Developing a model that is valid at any point in a

time-resolved simulation requires assumptions about these earlier pellet states. For example, in the current empirical fits for grain size evolution, a small variation in the initial grain diameter (from 10 to 11.7  $\mu\text{m}$ ) can result in the model predicting only grain shrinkage versus a combination of grain growth and shrinkage. Which of these is more correct remains an open question because grain growth has been widely characterized in an irradiated disk, which does not share the same radially changing characteristics as those of a proper fuel pellet.

It is known that HBS first forms on the periphery of the pellet, and a dark zone is formed partway through the pellet radius. This dark zone is characterized by an increase in pore area and an increased number of low-angle grain boundaries. Modeling the development of this region requires an understanding of the microstructure throughout the radius of the pellet throughout the irradiation lifetime. As such, there is a notable data gap for lower-burnup and fresh fuel microstructural characterization that would significantly improve the ability to model  $\text{UO}_2$  fuel restructuring.

To perform next steps in developing material models and increasing understanding of the evolution of  $\text{UO}_2$  fuel microstructure, it is necessary to perform additional characterization on fuel that has not been irradiated to HBU. These data will be used both to increase qualitative understanding of the fuel degradation and to model fuel performance.

In addition to data needs associated with the development of material models, there is the potential for additional examination of existing available fuel pellets. To date, microscopy has been performed on pre- and post-LOCA tested  $\text{UO}_2$  fuel pellets from North Anna. LOCA testing on these pellets was performed at SATS, and plans for tests of additional HBU fuel pellets involve a fall 2023 schedule. Radially resolved data have been reported on pore size and number density, grain size, and high- and low-angle grain boundary length per unit area for as-irradiated fuel for both NA1 and NA2, whereas post-LOCA data are incomplete (reported only partially for NA1 and not at all for NA2 pellets). Continuing examination of the fuel that has already undergone LOCA testing is a notable priority for expanding the available data for post-LOCA conditions.

Furthermore, there is the potential for performing TKD on the existing samples to gain additional insight into the fuel microstructure through the grain misorientation. There is also motivation to perform additional characterization on the cavities observed within the fuel. As previously mentioned, the tears within the fuel observed post-LOCA testing are assumed to form larger cavities and have a denuded zone around their periphery. Improved characterization of these phenomena will provide worthwhile insight into relatively unexplored behaviors in  $\text{UO}_2$  microstructural evolution with the use of fuel that has previously been irradiated and undergone LOCA testing, without additional testing required before characterization.

## **6. SUMMARY AND FUTURE WORK**

A desire to increase fuel burnup to decrease the cost of nuclear power plants has initiated a significant interest within the nuclear industry to develop improved understanding of HBU nuclear fuel microstructure and the potential for FFRD that contribute to burnup and safe operating limits. This milestone report describes joint research activities and program planning to develop mechanistic models for HBU  $\text{UO}_2$  microstructure, including both intra- and intergranular gas bubble populations and FGR, specifically associated with transient release. This model development is being leveraged extensively against a rapidly growing experimental database of high-fidelity electron microscopy characterization of commercial LWR fuel in the as-irradiated condition as well as that following simulated LOCA test conditions. This report describes the current status of model development, highlights recent microstructural data, and summarizes the data needs to complete the initial development and experimental validation of mechanistic models of FG and microstructural evolution at HBU and tFGR. In particular,

the distribution of FG bubbles within grains, on dislocation networks, and on grain boundaries should be considered. This consideration should include separating bubbles into populations of different sizes, depending on microstructure location (intra- or intergranular bubbles or bubbles pinned at dislocations). The number density and pressure of each bubble population should be tracked to link them to fragmentation. Such an activity involves both mesoscale and engineering-scale model development, combined with extensive experimental characterization of the HBU fuel microstructure, including bubbles, second phase precipitates, dislocations, and the grain structure, along with efficient data analysis to enable the cross-comparison and validation of models. The bubble populations must eventually be tracked at the fuel performance level, but the simplifications necessary at the engineering scale should be verified by mesoscale simulations.

## 7. REFERENCES

- Blondel, S., D. E. Bernholdt, K. D. Hammond, and B. D. Wirth. 2018. “Continuum-scale modeling of helium bubble bursting under plasma-exposed tungsten surfaces.” *Nuclear Fusion* 58 (12): 126034. <https://doi.org/10.1088/1741-4326/aae8ef>.
- Capps, N., L. Aagesen, D. Andersson, O. Baldwin, W. Cade Brinkley, M. W. D. Cooper, J. Harp, S. Novascone, P.-C. A. Simon, C. Matthews, and B. D. Wirth. 2023. “Empirical and mechanistic transient fission gas release model for high-burnup LOCA conditions.” *Journal of Nuclear Materials* 563: 154557.
- Electric Power Research Institute (EPRI). 2019. *Accident-Tolerant Fuel Valuation: Safety and Economic Benefits*. Revision 1, 3002015091.
- Lassmann, K., C. O’Carroll, J. van de Laar, and C. Walker. 1994. “The radial distribution of plutonium in high burnup  $\text{UO}_2$  fuels.” *Journal of Nuclear Materials* 208 (3): 223–231. ISSN: 0022-3115. [https://doi.org/10.1016/0022-3115\(94\)90331-X](https://doi.org/10.1016/0022-3115(94)90331-X).
- Lieou, C. K., N. A. Capps, M. W. D. Cooper, P.-C. A. Simon, and B. D. Wirth. 2023. “An integrated statistical-thermodynamic model for fission gas release and swelling in nuclear fuels.” Submitted to *Journal of Nuclear Materials*.
- Matthews, C., R. Perriot, M. W. D. Cooper, C. R. Stanek, D. A. Andersson. 2019. “Cluster dynamics simulation of uranium self-diffusion during irradiation in  $\text{UO}_2$ .” *Journal of Nuclear Materials* 527: 151787. ISSN 0022-3115, <https://doi.org/10.1016/j.jnucmat.2019.151787>.
- McKinney, C., R. Seibert, J. Werden, et al. 2023. “Characterization of the radial microstructural evolution in LWR  $\text{UO}_2$  using electron backscatter diffraction.” *Journal of Nuclear Materials* 585: 154 605. ISSN: 0022-3115. <https://doi.org/10.1016/j.jnucmat.2023.154605>.
- Noirot, J., Y. Pontillon, S. Yagnik, J. A. Turnbull, T. Tverberg. 2014. “Fission gas release behaviour of a 103 GWd/tHM fuel disc during a 1200°C annealing test.” *Journal of Nuclear Materials* 446: 163–171.
- Nuclear Energy Institute (NEI). 2019. *The Economic Benefits and Challenges with Utilizing Increased Enrichment and Fuel Burnup of Light-Water Reactors*.
- Pastore, G., L. Luzzi, V. Di Marcello, P. Van Uffelen. 2013. “Physics-based modelling of fission gas swelling and release in  $\text{UO}_2$  applied to integral fuel rod analysis.” *Nuclear Engineering and Design* 256: 75–86. <https://doi.org/10.1016/j.nucengdes.2012.12.002>.
- Raynaud, P. A. C. 2012. *Fuel Fragmentation, Relocation, and Dispersal during the Loss-of-Coolant Accident*. NUREG-2121.
- Rondinella, V. V. and T. Wiss. 2010. “The high burn-up structure in nuclear fuel.” *Materials Today* 13 (12): 24–32. ISSN 1369–7021, [https://doi.org/10.1016/S1369-7021\(10\)70221-2](https://doi.org/10.1016/S1369-7021(10)70221-2).
- Seibert, R., C. McKinney, C. Parish, et al. 2022. “Advanced microscopy characterization of high burnup commercial  $\text{UO}_2$  fuel before and after LOCA testing.” ORNL/SPR-2022/2618. Oak Ridge National Lab, Oak Ridge, TN. <https://info.ornl.gov/sites/publications/Files/Pub185202.pdf>.
- Seibert, R., N. Capps, J. Harp, J. Werden, C. Parish, and T. J. Gerczak. 2022. “Initial microstructure examination of high burnup fuel with varying operational histories.” *Oak Ridge Natl. Lab. Rep.*, p. ORNL/ 2022/2 SPR503.
- Tonks, M. R., D. Gaston, P. C. Millett, D. Andrs, P. Talbot. 2012. “An object-oriented finite element framework for multiphysics phase field simulations.” *Comput. Mater. Sci.* 51: 20.

- US Code of Federal Regulations (CFR). “Acceptance criteria for emergency core cooling systems for light-water nuclear power reactors,” Title 10, Part 50, Section 46, January 1974 (amended).
- US Nuclear Regulatory Commission (NRC). 2011. “Resolution of Generic Safety Issues.” NUREG-0933, Main Report with Supplements 1–33, Washington, DC.
- US Nuclear Regulatory Commission (NRC). 2017a. “Acceptance Criteria for Emergency Core Cooling Systems for Light Water Nuclear Power Reactors.” 10 CFR 50.46, Washington, DC.
- US Nuclear Regulatory Commission (NRC). 2017b. “Accident Source Term.” 10 CFR 50.67, Washington, DC.
- US Nuclear Regulatory Commission (NRC). 2021. *Interpretation of Research on Fuel Fragmentation Relocation and Dispersal at High Burnup*. RIL 202, 1–13.
- Wiesenack, W. 2013. *Summary of the Halden Reactor Project LOCA Test Series IFA-650, OECD Halden Reactor Project*. HPR-380.
- Wiesenack, W. 2015. *Summary and comparison of LOCA tests with BWR fuel in the Halden Reactor Project Test Series IFA-650*. OECD Halden Reactor Project, HPR-383.



